

CONDENSED
MATTER

Effect of Electron Delocalization on the “Recoil-Free” Absorption of γ -Ray Photons in $\text{Fe}_{1.75}\text{V}_{0.25}\text{BO}_4$ Warwickite

Yu. V. Knyazev^{a,*}, O. A. Bayukov^a, M. S. Shustin^a, D. V. Balatskii^b, N. A. Bel'skaya^c,
S. A. Gromilov^d, A. S. Sukhikh^d, V. V. Rudenko^a, and N. V. Kazak^{a,**}

^a Kirensky Institute of Physics, Federal Research Center KSC, Siberian Branch,
Russian Academy of Sciences, Krasnoyarsk, 660036 Russia

^b Institute of Chemistry, Far Eastern Branch, Russian Academy of Sciences, Vladivostok, 690022 Russia

^c Reshetnev Siberian State University of Science and Technology, Krasnoyarsk, 660037 Russia

^d Nikolaev Institute of Inorganic Chemistry, Siberian Branch, Russian Academy of Sciences,
Novosibirsk, 630090 Russia

*e-mail: yuk@iph.krasn.ru

**e-mail: nat@iph.krasn.ru

Received December 25, 2020; revised January 12, 2021; accepted January 13, 2021

Mössbauer spectroscopy is used to study the characteristic features of the crystal lattice dynamics in powdered single crystals of $\text{Fe}_{1.75}\text{V}_{0.25}\text{BO}_4$ warwickite in the temperature range of 4.2–505 K. The Debye temperature ($\Theta_D = 260$ K) is determined from the temperature dependence of the probability of the Mössbauer effect in the thin absorber approximation. It is found that the electron delocalization related to the fast electronic transfer between neighboring Fe^{3+} and Fe^{2+} cations takes place in the temperature range of 260–505 K. As a result, iron cations exhibiting the mixed valence ($\text{Fe}^{2.5+}$) arise. This process correlates with a change in the elastic properties of the lattice. Such correlation leads to a sharp decrease in the recoil-free absorption of γ -ray photons by the crystal lattice in the range of 260–400 K.

DOI: 10.1134/S002136402104010X

1. INTRODUCTION

In the first decades after R. Mössbauer's discovery of the effect of recoil-free absorption of gamma-ray photons [1, 2], a large number of experiments aimed at the study of the crystal lattice dynamics in solids were carried out [3–7]. The direct correlation between the phonon spectrum of a material and the probability of the recoil-free absorption of gamma-ray photons by the crystal lattice is described by the Debye model and can be expressed in terms of the well-known relation [8]

$$f = \exp \left[-\frac{3}{4} \frac{E_\gamma^2}{Mc^2 k_B \Theta_D} \times \left(1 + 4 \left(\frac{T}{\Theta_D} \right)^2 \int_0^{\frac{\Theta_D}{T}} \frac{x dx}{e^x - 1} \right) \right]. \quad (1)$$

Here, M is the mass of the ^{57}Fe atom, c is the speed of light in vacuum, k_B is the Boltzmann constant, E_γ is the energy of a gamma-ray photon (14.4 keV for ^{57}Fe), Θ_D is the Debye temperature, and $x = \hbar\omega/k_B T$ (\hbar is the Planck constant and ω is the frequency of elastic

vibrations). The expression for the absorption probability involves the Debye temperature Θ_D ; therefore, Mössbauer spectroscopy can be used to analyze structural phase transitions of different orders.

The most noticeable example of the application of Mössbauer spectroscopy for the analysis of local lattice dynamic processes is the study of BaTiO_3 perovskite near the ferroelectric transition [9]. It was shown that a sharp change in the probability of a recoil-free process near the phase transition point is due to small displacements of Ti atoms inside the oxygen octahedra. This gives rise to transverse phonon modes with anomalously low energies. An increase in the probability of excitation of such phonon vibrations results in a decrease in the probability of the Mössbauer effect [3, 10].

Studies of recoil-free absorption near magnetic transitions are fewer [11–13]. Using the Mössbauer effect in metallic iron, the authors of [11] showed for the first time how magnetic interactions between iron atoms reduce the rms displacement of atoms and sharply increase the probability of recoil-free absorption.

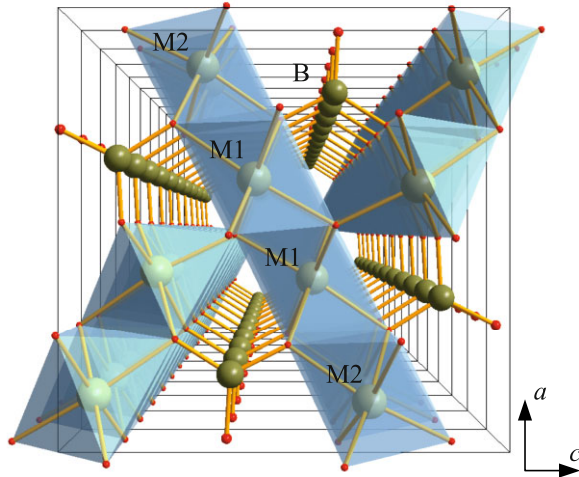


Fig. 1. (Color online) Crystal structure of $\text{Fe}_{1.75}\text{V}_{0.25}\text{BO}_4$ warwickite projected on the ac plane. Nonequivalent M1 and M2 crystallographic positions and boron atoms are indicated. Oxygen atoms are located at the apices of octahedra.

Despite the aforementioned achievements, the authors of recent work [14] wrote: “Among other experimental techniques that are able to measure local properties of the ferroelectric and antiferroelectric phase transitions, Mössbauer spectroscopy seems to be a forgotten technique.” The further advances in the Mössbauer technique are related to synchrotron radiation sources [15, 16]. For example, the inelastic scattering by nuclei makes it possible to study in detail the elastic characteristics of materials using the direct measurements of phonon spectra [17–19].

In this work, we study the characteristic features of the crystal lattice dynamics in the temperature range of 4.2–505 K for the powdered $\text{Fe}_{1.75}\text{V}_{0.25}\text{BO}_4$ single crystal having the warwickite structure using the Mössbauer spectroscopy technique. This material is characterized by two nonequivalent crystallographic positions occupied by transition metal atoms. At these positions, the degrees of distortion of the local environment are different; therefore, their contributions to the elastic properties of the crystal can be quite different.

The sample under study is promising for application in energy storage devices. The study of the electrochemical characteristics reveals the high efficiency of FeVBO_4 -based composites as anode materials [20]. The characterization of the magnetic and electrical properties of $\text{Fe}_{1.91}\text{V}_{0.09}\text{BO}_4$ single crystals with a low doping level is described in [21]. The room temperature Mössbauer spectroscopy reveals iron cations with the mixed-valence state ($\text{Fe}^{2.5+}$) similar to those in Fe_2BO_4 [22]. Here, it is important to note that

undoped Fe_2BO_4 is studied quite well [22–27] and it has very interesting electronic and magnetic characteristics. Below $T = 317$ K, electrons in Fe_2BO_4 are localized at iron cations with the formation of two charge states Fe^{2+} and Fe^{3+} . In this case, Fe^{2+} cations prefer the crystallographic positions in compressed octahedra (M2), whereas Fe^{3+} cations are located at the M1 positions (Fig. 1). This preference for heterovalent cations to occupy nonequivalent positions is referred to as charge ordering [22, 25]. As a result, an incommensurate superstructure consisting of electric dipoles is formed [25, 26]. It is well known that charge ordering under certain conditions gives rise to ferroelectricity [28]. The crystal lattice dynamics of such materials deserves a more thorough study.

2. SAMPLES AND METHODS

$\text{Fe}_{1.75}\text{V}_{0.25}\text{BO}_4$ warwickite single crystals were grown by the solution–melt method. The technique is described in detail in [21]. The X-ray structural analysis was performed using a Bruker X8 diffractometer (Mo $K\alpha$ radiation, graphite monochromator, ApexII CCD detector) at temperatures of 100 and 390 K. The sample temperature was controlled by a Cryostream 800Plus nitrogen flow cryostat (Oxford Cryosystems). The recording strategy involved standard $0.5^\circ \varphi$ and ω scans. The initial data acquisition, refinement of unit cell parameters, integration, and introducing the correction on absorption were performed using the Bruker Apex2 V.2013.6-2 software package (Bruker Advanced X-ray Solutions, Madison, Wisconsin, USA). The data set obtained was processed by employing the Olex2 v.1.2.10 software [29] with the SHELXT 2014/5 and SHELXL 2018/3 computer codes [30] used to determine the crystal structure and its refinement, respectively.

Mössbauer spectra were measured using powdered single crystals of $\text{Fe}_{1.75}\text{V}_{0.25}\text{BO}_4$ warwickite having a density of 7–10 mg/cm² according to the iron content. The measurements in the temperature range of 4.2–300 K were performed using an MS-1104Em spectrometer (Research Institute of Physics, Southern Federal University, Rostov-on-Don, Russia) in transmission geometry with a ^{57}Co (Rh) radioactive source (Ritverts company, Russia) using a CFSG-311-MESS cryostat with the sample in the gas-exchange chamber placed in a closed-loop cryogenic refrigerator implementing the Gifford–McMahon cycle. The recording of Mössbauer spectra in the high temperature range (350–505 K) was performed by a Wissel MB-550 spectrometer (Germany) in the transmission geometry with a ^{57}Co (Rh) γ -radiation source. A Wissel MBF-1100 furnace was used as a heater. The temperature control was performed using a TR-55 controller. The pressed-in sample was placed between two BN ceramic plates and was located in the glass cabin of the furnace.

The spectra were processed in two stages. At the first stage, the possible nonequivalent positions of iron in the sample were determined by calculating the probability distributions of quadrupole splitting and hyperfine fields. Using the results obtained, a preliminary model spectrum was designed. At the next stage, the model spectrum was fitted to the experimental one by varying the whole set of hyperfine parameters by the least squares method in the linear approximation. Further on, the values of chemical shifts are given relative to metallic iron (α -Fe).

3. RESULTS

The crystal lattice of the sample is shown in Fig. 1. The crystal lattice parameters and the unit cell volume are listed in Table 1. The complete set of crystallographic data is deposited in the database of the Cambridge Crystallographic Data Centre (<https://www.ccdc.cam.ac.uk/structures>), item nos. CCDC 2051305 (100 K) and CCDC 2051306 (390 K). Note here that $\text{Fe}_{1.75}\text{V}_{0.25}\text{BO}_4$ does not undergo any structural transitions, and the orthorhombic symmetry (space group $Pnma(62)$) is retained in the temperature range of 390–100 K. The refinement of occupancies revealed that the M1 and M2 sites are simultaneously occupied by iron and vanadium cations in the following ratios: M1 (0.87Fe + 0.13V) and M2 (0.88Fe + 0.12V).

The Mössbauer spectra of $\text{Fe}_{1.75}\text{V}_{0.25}\text{BO}_4$ obtained in the range of 4.2–505 K are shown in Fig. 2. The measurements in a wide temperature range allow studying the crystal lattice dynamics. However, we first consider some aspects of the fine structure of the sample.

Zeeman sextets appearing owing to magnetic ordering persist in the temperature range of 4.2–125 K. This is consistent with the ferrimagnetic ordering temperature ($T_N = 130$ K) determined from the magnetometric data [21]. At $T = 4.2$ K, the spectrum consists of four sextets, pairwise related to divalent ($IS \approx 1.2$ mm/s) and trivalent ($IS \approx 0.5$ mm/s) iron cations, occupying two crystallographically nonequivalent positions [31]. The sextet corresponding to divalent iron with strongly broadened lines and a low hyperfine field $H_{\text{hf}} = 140$ kOe is also observed. A similar value of the hyperfine field was observed in undoped Fe_2BO_4 [22, 32]. The state of iron with such a low value of the hyperfine field can be both a manifestation of strong covalent effects [33] and a result of geometric frustration, to which the structure of warwickite is highly susceptible [34]. Frustration is a property of the crystal structure of warwickite itself and can lead to the loss of the long-range magnetic order under certain conditions [31, 35].

Next, we will focus on the relationship between the charge and vibrational subsystems of $\text{Fe}_{1.75}\text{V}_{0.25}\text{BO}_4$. Above 135 K, the form of the Mössbauer spectra sug-

Table 1. Unit cell parameters for $\text{Fe}_{1.75}\text{V}_{0.25}\text{BO}_4$ at 100 and 390 K

T , K	100	390
a , Å	9.2410 (11)	9.255 (10)
b , Å	3.1672 (3)	3.1786 (14)
c , Å	9.3833 (12)	9.401 (4)
V , Å ³	274.63 (5)	276.6 (2)
Space group	$Pnma$	$Pnma$
Z	4	4

gests the existence of the paramagnetic state of the material. In the temperature range of 135–260 K, the spectra consist of four doublets, which, in terms of the chemical shift, correspond to divalent and trivalent iron cations in the octahedral oxygen environment. A further increase in the temperature gives rise to the mixed valence state of iron, $\text{Fe}^{2.5+}$ ($IS \approx 0.5$ – 0.7 mm/s). This state is due to the sharing of an electron between two neighboring iron cations at the M1 and M2 positions. According to our data, such a state exists over the whole temperature range above 260 K. If we compare this phenomenon with the Verwey transition in magnetite [36] and with the “charge ordering” in Fe_2BO_4 [22, 32], it worth mentioning that the Verwey transition and charge ordering in Fe_2BO_4 are accompanied by anomalies in the electrical conductivity, which are not found in the doped warwickite [21].

At a given temperature, the area under the spectral curve is equivalent to the magnitude of the Mössbauer effect. Therefore, to estimate this magnitude, we use the integration of the accumulated signal corresponding to resonant γ -ray photons over all channels of the analyzer in the Mössbauer spectrometer, taking into account the spectral background. By normalizing the found values to the area at 4.2 K (A_0), we obtain the temperature dependence of the relative magnitude of the effect A/A_0 , which is shown by circles in Fig. 3. Taking the logarithm of Eq. (1) in the temperature range $T > \Theta_D/2$, we obtain the expression determining the Debye temperature [7, 37, 38]

$$\frac{d \ln f}{dT} \propto \frac{d \ln A}{dT} = -\frac{3E_\gamma^2}{Mc^2 k_B \Theta_D^2}. \quad (2)$$

Then, the Debye temperature determined from Eq. (2) is $\Theta_D = 260$ K. This temperature is somewhat lower than Θ_D for other crystals with the warwickite structure [39, 40]. Thus, a certain “softening” of the lattice occurs, in contrast, for example, to the substitution of S atoms for Se in $\text{FeSe}_{0.91}\text{S}_{0.09}$, which leads to the doubling of Θ_D [41].

Using the value of Θ_D , one can estimate some parameters characterizing the elastic properties of the crystal. Thus, according to the definition of Θ_D , the

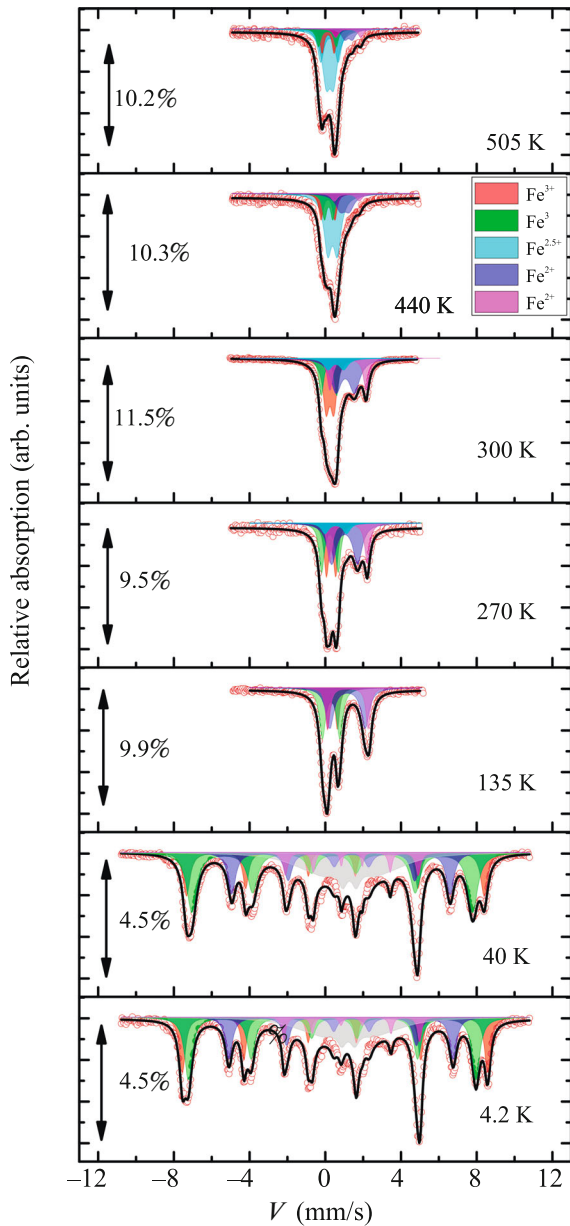


Fig. 2. (Color online) Mössbauer spectra of $\text{Fe}_{1.75}\text{V}_{0.25}\text{BO}_4$ measured in the temperature range of 4.2–505 K. Experimental data are shown by circles. Solid curves illustrate the results of fitting the spectra.

maximum frequency of phonon vibrations is $\omega_m = k_B\Theta_D/h = 3.62 \times 10^{13}$ Hz. The speed of elastic waves in the material, V_m , can be estimated using the expression

$\Theta_D = \frac{h}{k_B} \left[\frac{3q N_A \rho}{4\pi M} \right]^{1/3} V_m$ [42]. Here, q is the number of atoms in the basic chemical formula ($q = 7$ for $\text{Fe}_{1.75}\text{V}_{0.25}\text{BO}_4$), N_A is the Avogadro number, ρ is the density of the material (for $\text{Fe}_{1.75}\text{V}_{0.25}\text{BO}_4$, $\rho = 4.448$ g/cm³ according to the X-ray diffraction data),

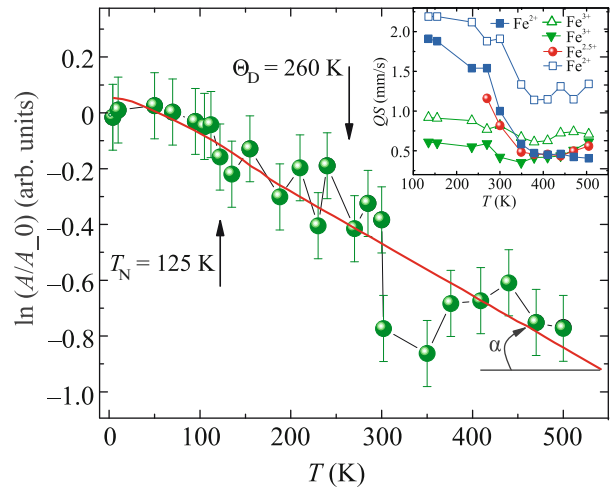


Fig. 3. (Color online) Temperature dependence of the probability of Mössbauer effect plotted on a logarithmic scale. The solid curve corresponds to the Debye model. The Θ_D value is determined from the slope of the solid curve $\tan\alpha = d\ln A/dT = 0.00201$. The temperature dependence of the quadrupole splitting of the spectral components is shown in the inset.

and M is the molar mass (186 g/mol). For the sample under study, the velocity of propagation for elastic vibrations is 1880 m/s, which is somewhat lower than that in the materials with the orthorhombic crystal lattice [42].

In the high-temperature range, a strong decrease in recoil-free absorption with the subsequent return to a linear dependence is observed. This process manifests itself in the temperature range of 260–505 K, which can be divided into two ranges: (i) 260–400 K, where the degree of electron delocalization increases slowly and correlates with the $QS(T)$ dependence illustrated in the inset of Fig. 3, and (ii) 400–505 K, characterized by a sharp increase in the degree of delocalization of an electron shared by iron atoms. This is well illustrated in Fig. 4 by the temperature dependence of the occupation of spectral components corresponding to different charge states.

In the first range, the $\ln(A/A_0)(T)$ dependence significantly deviates from the linear one predicted by the Debye model. This behavior of the magnitude of the Mössbauer effect is characteristic of ferroelectrics near the ferroelectric transition owing to the arising soft phonon modes and to the anharmonicity of atomic vibrations in the lattice [9, 14]. Since $\text{Fe}_{1.75}\text{V}_{0.25}\text{BO}_4$ does not exhibit any structural transition in the temperature range of 100–390 K, the sharp decrease in the probability of recoil-free absorption of γ -ray photons is possibly caused by the strong coupling of the electron and phonon subsystems. It is quite probable that the rearrangement of the spectrum of vibrational modes occurs in this range along with a change in the

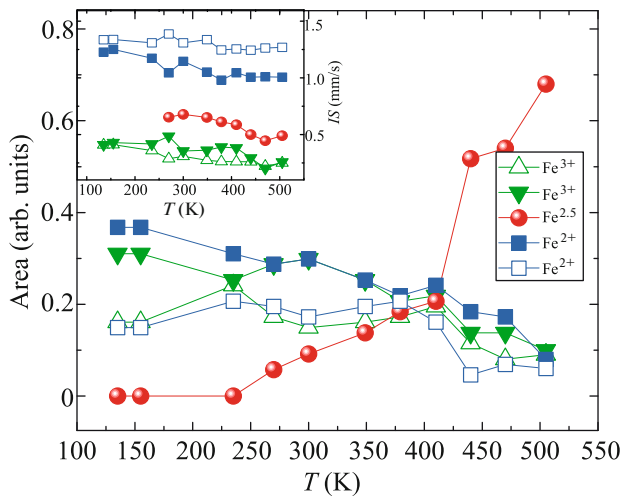


Fig. 4. (Color online) Temperature dependence of the occupation of different charge states of iron cations in $\text{Fe}_{1.75}\text{V}_{0.25}\text{BO}_4$. The temperature dependence of the isomer shift of spectral components is shown in the inset.

electronic structure upon sharing of electrons and the formation of the $\text{Fe}^{2.5+}$ states.

In the second specified range, the correspondence between the experimental and theoretical dependences of recoil-free absorption is restored. It is quite probable that all vibrational modes existing in the system are excited in this range. This allows us to assume that significant deviations of the $\ln(A/A_0)(T)$ dependence from the linear one occurring at 260–400 K are due to the rearrangement of the vibrational spectra. The features of the rearrangement of phonon spectra can be qualitatively understood by linear fits of the behavior in different temperature ranges between 260 and 505 K. Such fits would characterize the elastic parameters of the system in each range. In this approach, an increase in the slope angle (α) of the $\ln(A/A_0)(T)$ function in the temperature range of 260–400 K corresponds to a decrease in the rigidity of the lattice. Thus, the contribution of fast electron exchange has some characteristics of a phase transition occurring without changing the lattice symmetry and requires additional study. Apparently, electron sharing between iron atoms increases the occupation numbers of low-energy phonon modes, which determine the elastic properties of the lattice in this temperature range.

Note that the electron and phonon subsystems can affect each other in the process of mutual rearrangement of the electron structure and vibrational characteristics taking place in the temperature range of 260–505 K. On one hand, electron sharing between iron atoms can change the elastic properties of the lattice. On the other hand, vibrations (including anharmonic ones) of cations can lead to the equalization of the

electron energies at neighboring cations and contribute to the sharing of electrons.

4. CONCLUSIONS

Thus, using the Mössbauer spectroscopy data, we have determined the Debye temperature for $\text{Fe}_{1.75}\text{V}_{0.25}\text{BO}_4$ single crystals, $\Theta_D = 260$ K. The observed increase in the degree of electron sharing between neighboring iron cations is likely due to the temperature-induced lowering of the threshold for the excitation of fast electron exchange. The determined relationship between the electronic and vibrational subsystems can be caused both by a change in the elastic coupling in pairs of iron cations due to the electron sharing and by a strong electron–phonon interaction in the system. In the first case, the change in the phonon spectrum is only due to the specific features of the localized electron states, which, as we have already mentioned, was not observed. In the second case, the band states of electrons are involved and, as expected, this should lead to the modification of the conductivity of the material. Therefore, we believe that the strong coupling of the electron and phonon subsystems in the temperature range of $T = 260$ –400 K is due to a change in the elastic characteristics of the lattice, which is related to electron sharing. Note that the opposite effect is also possible: excited vibrations in the lattice (including anharmonic vibrations) can reduce the energy barrier between different electron states and equalize the energies of two neighboring sites and, consequently, favor electron sharing.

FUNDING

This work was supported by the Council of the President of the Russian Federation for Support of Young Scientists and Leading Scientific Schools (project no. MK-2339.2020.2) and by the Russian Foundation for Basic Research (project no. 20-02-00559-a).

REFERENCES

1. R. L. Mössbauer, *Naturwissenschaften* **45**, 538 (1958).
2. R. L. Mössbauer, *Z. Phys.* **151**, 124 (1958).
3. Č. Muzikář, V. Janovec, and V. Dvořák, *Phys. Status Solidi B* **3**, K9 (1963).
4. V. A. Bokov, V. P. Romanov, and V. V. Chekin, *Sov. Phys. Solid State* **7**, 1521 (1965).
5. V. Chekin, V. Romanov, B. Verkin, and V. Bokov, *JETP Lett.* **2**, 117 (1965).
6. T. Kobayashi and K. Fukumura, *Nucl. Instrum. Methods Phys. Res.* **180**, 549 (1981).
7. R. D. Ernst, D. R. Wilson, and R. Herber, *J. Am. Chem. Soc.* **106**, 1646 (1984).
8. M. Eibschütz, S. Shtrikman, and D. Treves, *Phys. Rev.* **156**, 562 (1967).
9. V. Bhide and M. Multani, *Phys. Rev. A* **139**, 1983 (1965).

10. A. Jain, S. Shringi, and M. Sharma, *Phys. Rev. B* **2**, 2756 (1970).
11. B. Kolk, A. Bleloch, and D. Hall, *Hyperfine Interact.* **29**, 1377 (1986).
12. J. Fontcuberta, *Phys. Status Solidi B* **139**, 379 (1987).
13. K. Sharma, V. R. Reddy, A. Gupta, S. Kaushik, and V. Siruguri, *J. Phys.: Condens. Matter* **24**, 376001 (2012).
14. M. Podgórna, J. Żukrowski, I. Jankowska-Sumara, A. Majchrowski, and K. Berent, *Phys. Status Solidi B* **254**, 1700137 (2017).
15. I. S. Lyubutin, S. Starchikov, A. G. Gavriluk, I. Troyan, Y. A. Nikiforova, A. Ivanova, A. Chumakov, and R. Ruffer, *JETP Lett.* **105**, 26 (2017).
16. Y. V. Knyazev, A. Chumakov, A. Dubrovskiy, S. V. Semenov, S. S. Yakushkin, V. Kirillov, O. N. Martyanov, and D. A. Balaev, *JETP Lett.* **110**, 613 (2019).
17. V. Belyakov, *JETP Lett.* **67**, 8 (1998).
18. A. Chumakov, A. Barla, R. Ruffer, J. Metge, H. Grünsteudel, H. Grünsteudel, J. Plessel, H. Winkelmann, and M. Abd-Elmeguid, *Phys. Rev. B* **58**, 254 (1998).
19. R. Pradip, P. Piekarz, D. G. Merkel, J. Kalt, O. Waller, A. I. Chumakov, R. Ruffer, A. M. Oleś, K. Parlinski, T. Baumbach, and S. Stankov, *Nanoscale* **11**, 10968 (2019).
20. M. Dong, Q. Kuang, X. Zeng, L. Chen, J. Zhu, Q. Fan, Y. Dong, and Y. Zhao, *J. Alloys Compd.* **812**, 152165 (2020).
21. A. Balaev, O. Bayukov, A. Vasilev, D. Velikanov, N. Ivanova, N. Kazak, S. Ovchinnikov, M. Abd-Elmeguid, and V. Rudenko, *J. Exp. Theor. Phys.* **97**, 989 (2003).
22. A. Douvalis, V. Papaefthymiou, A. Moukarika, T. Bakas, and G. Kallias, *J. Phys.: Condens. Matter* **12**, 177 (2000).
23. N. Suda, K. Kohn, and S. Nakamura, *Ferroelectrics* **286**, 155 (2003).
24. M. Sánchez-Andújar, J. Mira, B. Rivas-Murias, S. Yáñez-Vilar, N. Biskup, J. Rivas, and M. A. Señaris-Rodríguez, *IEEE Trans. Magn.* **44**, 2989 (2008).
25. M. Angst, P. Khalifah, R. Hermann, H. Xiang, M.-H. Whangbo, V. Varadarajan, J. W. Brill, B. C. Sales, and D. Mandrus, *Phys. Rev. Lett.* **99**, 086403 (2007).
26. S. Bland, M. Angst, S. Adiga, V. Scagnoli, R. Johnson, J. Herrero-Martin, and P. Hatton, *Phys. Rev. B* **82**, 115110 (2010).
27. H. Yang, H. Tian, Y. Song, Y. Qin, Y. Zhao, C. Ma, and J. Li, *Phys. Rev. Lett.* **106**, 016406 (2011).
28. J. van den Brink and D. I. Khomskii, *J. Phys.: Condens. Matter* **20**, 434217 (2008).
29. O. Dolomanov, L. Bourhis, R. Gildea, J. Howard, and H. Puschmann, *J. Appl. Crystallogr.* **42**, 339 (2009).
30. G. M. Sheldrick, *Acta Crystallogr. A* **71**, 3 (2015).
31. I. Lyubutin, N. Y. Korotkov, K. Frolov, N. Kazak, M. Platunov, Y. V. Knyazev, L. Bezmaternykh, S. Ovchinnikov, A. Arauzo, and J. Bartolomé, *J. Alloys Compd.* **642**, 204 (2015).
32. A. Douvalis, V. Papaefthymiou, A. Moukarika, and T. Bakas, *Hyperfine Interact.* **126**, 319 (2000).
33. G. Abramova, Y. Knyazev, O. Bayukov, and S. Kubrin, *Phys. Solid State* **63**, 68 (2021).
34. A. Akrap, M. Angst, P. Khalifah, D. Mandrus, B. C. Sales, and L. Forró, *Phys. Rev. B* **82**, 165106 (2010).
35. Y. V. Knyazev, N. Kazak, M. Platunov, N. Ivanova, L. Bezmaternykh, A. Arauzo, J. Bartolomé, and S. Ovchinnikov, *J. Alloys Compd.* **642**, 232 (2015).
36. E. Verwey, *Nature (London, U.K.)* **144**, 327 (1939).
37. R. H. Herber and D. Johnson, *Inorg. Chem.* **18**, 2786 (1979).
38. R. Giovanelli and A. Orefice, *Phys. Lett. A* **298**, 279 (2002).
39. M. Continentino, A. Pedreira, R. Guimaraes, M. Mir, J. Fernandes, R. Freitas, and L. Ghivelder, *Phys. Rev. B* **64**, 014406 (2001).
40. N. V. Kazak, M. S. Platunov, Y. V. Knyazev, N. B. Ivanova, O. A. Bayukov, A. D. Vasiliev, L. N. Bezmaternykh, V. I. Nizhankovskii, S. Y. Gavrilkin, K. V. Lamonova, and S. G. Ovchinnikov, *J. Magn. Magn. Mater.* **393**, 316 (2015).
41. K. V. Frolov, I. S. Lyubutin, D. A. Chareev, and M. Abdel-Hafiez, *JETP Lett.* **110**, 562 (2019).
42. O. L. Anderson, *J. Phys. Chem. Solids* **24**, 909 (1963).

Translated by K. Kugel